Hybrid AI-Thermal Model Trained via Monte Carlo Simulations to Study Self-Heating Effects

Sergio García-Sánchez, Ignacio Íñiguez-de-la-Torre,
Tomás González, *Senior Member, IEEE*, and Javier Mateos, *Member, IEEE*

***Abstract*—This paper presents a hybrid AI-thermal model for the determination of the current and lattice temperature of a device under a given bias voltage. The model is based on a neural network trained with isothermal Monte Carlo simulations and the coupling of any thermal model where the lattice temperature depends on the dissipated power. The proposed procedure has been validated on a GaN-based self-switching diode, although its application to other electronic devices such as transistors is also straightforward. The proposed method allows for a significant reduction in computational cost, in addition to enabling the investigation of various thermal models in an efficient manner. It is capable of reproducing the results that would be obtained through electrothermal Monte Carlo simulations, which are particularly computationally expensive.**

***Index Terms*—Monte Carlo Simulations, Artificial Intelligence (AI), Thermal models, Artificial Neural Networks (ANN), GaN, Electronic devices**

I. Introduction

In just a short time, devices based on nitrides, such as Gallium Nitride (GaN), have become ideal candidates for operation at high temperatures and high output power [1], [2], [3], [4]. One of the most important aspects leading to the degradation of the devices is the elevated temperature reached inside, being self-heating a major limitation because the high-power dissipation [4], [5], [6]. The use of thermal models has become very useful in electronic device simulations to obtain the temperature distribution within the device and its impact on performance [1], [5], [7], reliability [6], and lifespan [8], [9]. Also, thermal models are essential for determining temperature limits, helping to prevent device breakdown, and thereby avoiding unnecessary manufacturing costs. Commercial software and home-made simulators include thermal effects via different alternatives, going from simple models based on a thermal resistance and the dissipated power (P_{diss}) inside the device [10], [11], [12] to others that take into account the heat diffusion equation (HDE) [13], [14], [15], and those that employ the Boltzmann equation for phonons [16].

This work has been partially supported through grants PID2020-115842RB-I00 and PDC2023-145896-I00 funded by MCIN/AEI/10.13039/501100011033, the Junta de Castilla y León and FEDER through project SA136P23 and the Fundación General de la Universidad de Salamanca through project PC_TCUE23-24_011. This research has made use of the high performance computing resources of the Castilla y León Supercomputing Center (SCAYLE, www.scayle.es), financed by the European Regional Development Fund (ERDF). (*Corresponding author: Sergio García-Sánchez*)

S. García-Sánchez, I. Íñiguez-de-la-Torre, T. González and J. Mateos are with with the Applied Physics Department, and USAL-NANOLAB, Universidad de Salamanca, 37008 Salamanca, Spain (e-mail: sergio_gs@usal.es, indy@usal.es, tomasg@usal.es and javierm@usal.es).

Electrothermal simulations can be computationally expensive, meaning they require a significant amount of computation time as well as computational resources. In this context, Artificial Intelligence (AI) techniques have emerged as a powerful tool to reduce the costs associated with modeling electronic devices [17], [18], [19] or electronic systems [20]. Machine Learning (ML) algorithms, such as Artificial Neural Networks (ANN), are used for regression analysis, predicting an output variable (numeric dependent variable) based on a set of input variables (numeric independent variables) [21]. On the other hand, ANNs are an attractive option compared to other regression techniques, such as, for example, linear regression, decision trees or Support Vector Machines (SVM) due to the advantages they present. Specifically, they generally allow greater flexibility in the representation of data, capturing non-linear and complex relationships between input and output variables more accurately than linear methods such as linear regression [22], [23]. In addition, neural networks allow us to generalize well from training data to make accurate predictions on unseen vales and their algorithms allow the automation of the modeling process, which leads to savings in time and resources [23].

In previous works, through an electrothermal MC simulator, self-heating was successfully studied in Self-Switching Diodes (SSDs) [12] and High Electron Mobility Transistors (HEMTs) [24]. However, this procedure is tedious since the simulations require high computational cost and, for each modification of each parameter of the thermal model, a complete MC simulation is required. In this work we present a method to reduce this computational cost by combining a neural network (trained with data from isothermal MC simulations) and different thermal models. With the proposed technique it is possible to determine, without performing electrothermal MC simulations, the current density and the lattice temperature (T_{latt}) of the device for specific bias conditions and device properties. Although in this study we focus on a planar nanodiode to be used as Gunn diode [25], the technique to be described could be applied to other types of devices.

The paper is structured as follows. First, the details of the device that has been selected as case study and the home-made MC simulator are presented. Then, the developed ANN is explained, together with the metrics that validate the good accuracy of the model. The next section presents the proposed method, a combination of a predictive network and any thermal model where T_{latt} depends on P_{diss}. In our case, the technique will be applied to three thermal models, which are briefly described in Section IV(A). The results are presented in

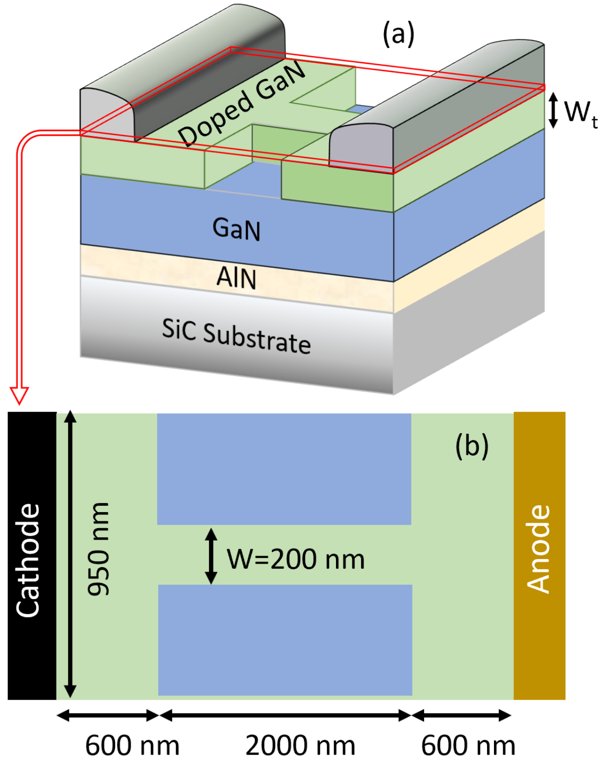

Fig. 1. (a) 3D structure of the doped-GaN diode. (b) Top-view structure used in the 2D MC simulations.

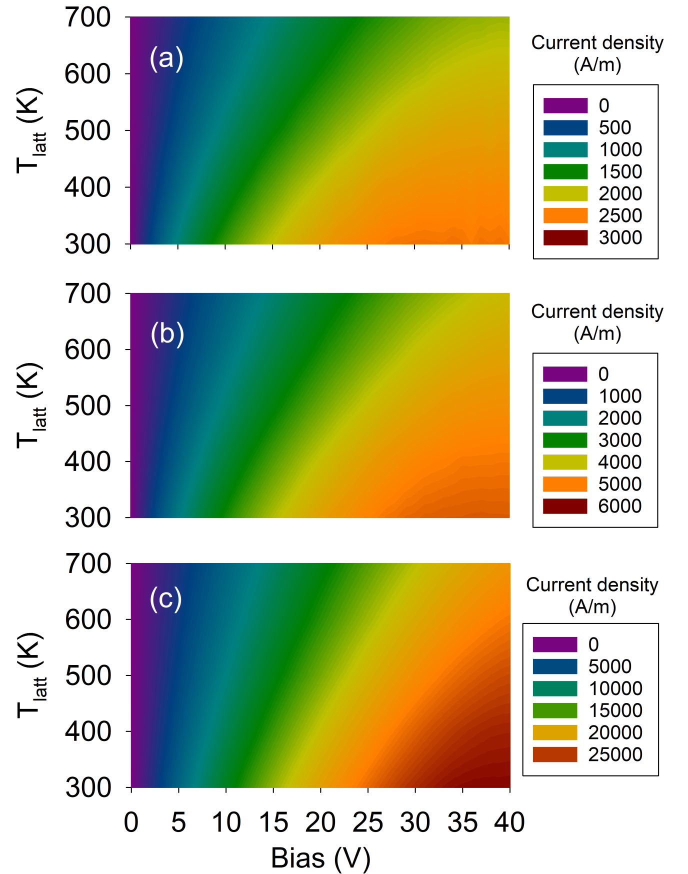

Fig. 2. Maps of current density as a function of the applied cathode-to-anode voltage, V, and lattice temperature, T_{latt}: (a) N_D=0.5×10^{24} m^{-3}, (b) N_D=1.0×10^{24} m^{-3} and (c) N_D=5.0×10^{24} m^{-3}.

Section IV(B) and finally the main conclusions of the work are provided.

II. DEVICE DETAILS AND MONTE CARLO SIMULATIONS

The schematic structure of the doped-GaN diode studied in this paper is shown in Fig. 1(a). It is a planar diode where the top doped GaN layer is etched to form insulating trenches. The dielectric permittivity within the trench region is defined as $\varepsilon_r = 1$ (air). We perform MC simulations of the top region, denoted as top-view simulations, whose schema is depicted in Fig. 1(b). The diode has a length of the active region of 2000 nm, and a channel width of 200 nm. The doping of the GaN layer (N_D) and T_{latt} will be within the 0.5-10×10^{24} m^{-3} and 300 K-700 K ranges, respectively. We will provide values of current density (in A/m), to be multiplied by the thickness of the top doped GaN layer (W_t) to obtain the current (in A) flowing in a concrete device.

The simulation tool employed for the study of the devices is a home-made semiclassical ensemble MC simulator self-consistently coupled with a two-dimensional resolution of the Poisson's equation [26], [27], [28], [29]. The simulator takes into account the following scattering mechanisms: intervalley, acoustic and optical (polar and non-polar) phonons, piezo-electric and ionized impurities. Equilibrium Bose-Einstein occupation for phonons is always employed. The inclusion of non-equilibrium phonon distributions would affect both the electron transport in the devices and and their thermal resistance, but the global framework presented here would remain the same.

The conduction bands of materials are modelled by a three-nonparabolic, spherical valley model [30] and, for GaN, the Wurzite structure is considered [26], [31]. The lowest point of the conduction band of GaN is located at the Γ point (Γ_1-valley), 3.44 eV above the absolute maximum of the valence band, also located at the Γ point. The second minimum is located between the M and L points, leading to a valley called the U-valley. An energy separation to the first to second valley of ε_{1-2}=0.9 eV [32], [33], [34] is contemplated in our model. The third minimum is also in the Γ point, the Γ_3-valley, at 2.4 eV from the minimum of the Γ_1-valley. We want to highlight that most simulations of GaN devices —except for the model employed by Sadi *et al.* [35] for MC simulations of LEDs— typically use ε_{1-2}=2.2 eV. This value is derived from Density Functional Theory (DFT) calculations [36] and other similar theoretical works [37], [38]. However, recent experimental findings indicate that ε_{1-2} for GaN could be lower, approximately ε_{1-2}=0.9 eV [32], [33], [34]. Some authors have acknowledged the controversy between theoretical predictions and measurements but opted to discard the experimental value [39]. In our case, we have chosen to use this lower intervalley separation ε_{1-2}=0.9 eV because MC simulations of Gunn diodes using this value show a good correlation between the threshold voltage for the onset of Gunn oscillations and the experimental breakdown voltage, which

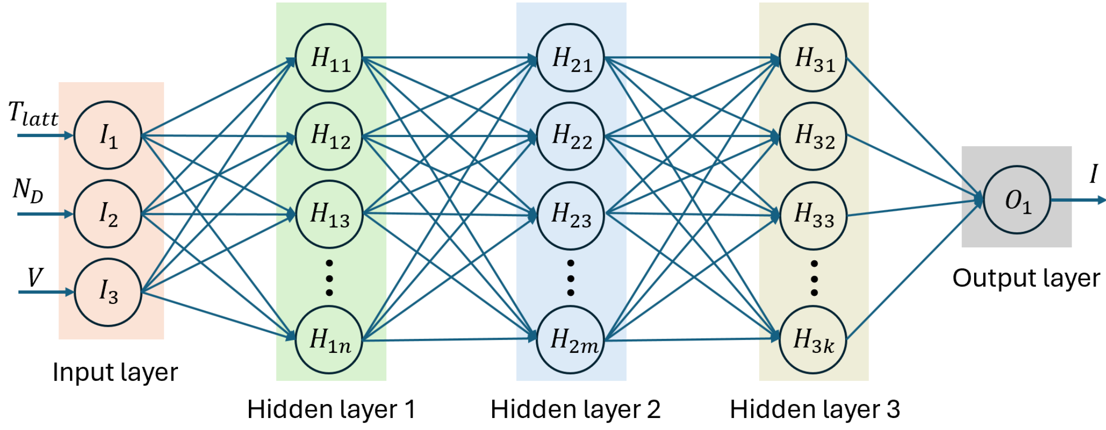

Fig. 3. Schematic diagram of the deep neural network comprised of an input layer, three hidden layers and an output layer. Lattice temperature (T_{latt}), doping, (N_D) and bias (V) are the input variables and the current density (I) is the target variable.

we believe appear at the same time [25]. Additionally, the simulator takes into account a self-consistent surface-charge model as described in Ref. [40].

The maps of Fig. 2 represent results of isothermal MC simulations used for the training and validation of the network. In particular, we show the current density (I) as a function of the applied bias (V) and T_{latt} for three values of the doping N_D. As observed, the current density is essentially proportional to N_D and is strongly influenced by T_{latt}. When T_{latt} increases, electron-phonon scattering is enhanced, which reduces the current level. Remarkable levels of heat dissipation due to the Joule effect can be reached in these highly-doped devices when increasing the applied voltage. According to the results in Fig. 2, the associated increase of T_{latt} cannot be ignored to evaluate the current density. Thus, it is essential to account for self-heating in the analysis of these devices.

III. ARTIFICIAL NEURAL NETWORK MODEL

The ANN used in this paper is a multilayer perceptron, [41], a neural network in which every node is connected to each layer's next node. The determination of the number of hidden layers and the number of neurons in each hidden layer are hyperparameters that need to be decided during the model design phase, and may vary depending on the specific problem being addressed [42]. To capture the non-linear relationship between the input and output variables, it is advisable to include one or more hidden layers [43]. The number of neurons in hidden layers has been determined such as three times the size of the input layer, plus the size of the output layer [43], [44]. The schema of the ANN used is shown in Fig. 3. The ANN is made up of three hidden layers with 10 neurons each, and it considers as input variables V, N_D, and T_{latt}. The ANN provides the prediction of I, our target variable. For training our ANN, the backpropagation algorithm has been adopted, using the $neuralnet$ function from the package $neuralnet$ in the R statistical software programming language [45]. The dataset has been split into train and validation sets accordingly the proportion of 80 % and 20 %, respectively, taking into account that validation data are not present during the training of the model. Variables have been previously rescaled by the min-max normalization method [46] accordingly to the formula:

$$x' = \frac{x - min(x)}{max(x) - min(x)}, \tag{1}$$

where x is the original value, x' the normalized value, and $min(x)$ and $max(x)$ the minimum and maximum values of x, respectively. The convergence criteria for training the ANN (threshold parameter in the neuralnet function) has been configured to 0.0001. For the training and validation of the ANN a total of 820 simulations were used considering biases in the 0 V-40 V range, lattice temperatures in the 300 K-700 K range, and doping levels in the 0.5-10$\times 10^{24}$ m^{-3} range. Taking into account the high computational cost of each MC simulation (around 144 hours), special care has been taken to include the smallest number of MC simulations without the model having underfitting. There are several statistical metrics that are used for evaluating the accuracy of regression models, in particular, the Root Mean Squared Error ($RMSE$) and the Mean Absolute Error (MAE) [47], [48].

The $RMSE$ gives the average prediction error made by the model, where a value of zero would indicate a perfect fit to the data and it is defined accordingly as:

$$RMSE_{(y,\hat{y})} = \sqrt{\frac{\sum_{i=1}^{N}(y_i - \hat{y}_i)^2}{N}}, \tag{2}$$

where y_i is the actual value of the ith observation, $\hat{y}_i$ the value of the ith prediction, and N the number of observations.

The MAE gives the absolute difference between the actual values and the values predicted by the model for the target variable and a value of of zero would mean a perfect prediction and it is defined by:

$$MAE_{(y,\hat{y})} = \frac{1}{N}\sum_{i=1}^{N}|y_i - \hat{y}_i|, \tag{3}$$

The $RMSE$ and MAE values for training and validation are summarized in Table. I. The obtained $RMSE$ and MAE

statistics show the good accuracy of the ANN to predict the target (close to zero value and there is not a remarkable difference between the training and validation score), which indicates that the model is goodfitting.

TABLE I
STATISTICS OF THE VALIDATION RESULTS FOR TRAINING AND VALIDATION: N, $RMSE$ AND MAE.

	N	$RMSE$	MAE
Training	655	0.0011	0.0008
Validation	165	0.0013	0.0009

In order to validate the prediction, Fig. 4 shows the $I-V$ characteristics for a diode with a doping of N_D=5×10^{24} m^{-3}, at lattice temperatures of 300 K, 400 K, 500 K, 600 K, and 700 K obtained by MC simulations (symbols) and by the constructed ANN (lines). As can be seen, a very good fit between simulations and predictions is found.

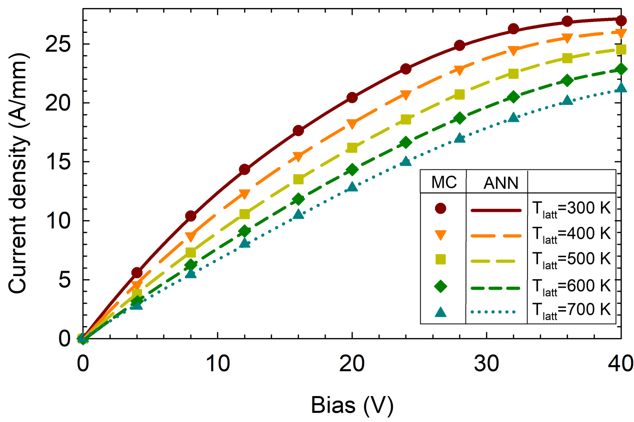

Fig. 4. *I-V* characteristics obtained from (symbols) MC simulations and (lines) ANN model for the lattice temperatures of 300 K, 400 K, 500 K, 600 K and 700 K. N_D=5×10^{24} m^{-3}.

IV. COMBINED ARTIFICIAL NEURAL NETWORK AND THERMAL MODEL

In Fig. 5 the flux diagram of the operation of the hybrid AI-thermal model is depicted. The first iteration starts with T_{latt}=T_0 (300 K in our case) and, using the ANN model, I_0 is predicted for the desired doping N_D and applied voltage V. Then, an iterative computation starts. The lattice temperature corresponding to the current predicted by the ANN, T_{latt}^{i+1}, is calculated based on a given thermal model (TRM) using the value of the dissipated power $P_{diss.i}$=I_i×V. If T_{latt}^{i+1} is different from T_{latt}^{i}, a new current prediction would be performed for this new T_{latt}^{i+1}. Once T_{latt} converges ($T_{latt}^{i+1} \approx T_{latt}^{i}$) the program terminates. At this point, T_{latt} and I are the values provided by our combined model for the given N_D and V, and the considered (TRM). This procedure is versatile and allows applying any thermal model whose temperature depends on the value of P_{diss}. Next, three thermal models are presented, all based on a thermal resistance.

A. THERMAL MODELS

Different relationships between the T_{latt} and P_{diss} can be considered [12]. The first approach used in this study is based on an ad-hoc temperature-independent thermal resistance ($TRM1$), R_{th} [11], [12], where T_{latt} is obtained according to:

$$TRM1: T_{latt} = T_{amb} + P_{diss} \times R_{th}, \tag{4}$$

being T_{amb} the temperature of the heat sink.

The second approach ($TRM2$) employs a temperature dependent thermal resistance, where R_{th} is considered as a function of T_{latt} according to [49]:

$$R_{th}(T_{latt}) = R_{th}\left(\frac{T_{latt}}{T_{amb}}\right)^{\alpha_{eff}}, \tag{5}$$

being R_{th} the thermal resistance at T_{amb}, and α_{eff} an adjustable parameter since typically the device structure comprises different materials with different temperature dependencies of thermal conductivity [13], [14], [15]. To calculate T_{latt} the Kirchhof variable transformation [13], [14], [15] is applied, obtaining:

$$TRM2: T_{latt} = T_{amb} \times \left[1 + \frac{P_{diss} \times R_{th}(1-\alpha_{eff})}{T_{amb}}\right]^{\frac{1}{1-\alpha_{eff}}}, \tag{6}$$

Thirdly, a non-linear thermal resistance model ($TRM3$) can be used to reproduce the non-linear behaviour of the thermal resistance [27], where T_{latt} is obtained taking into account an extra term as:

$$TRM3: T_{latt} = T_{amb} + P_{diss} \times R_{th}\left(1 + \left[\frac{P_{diss} \times R_{th}}{\Delta T_0}\right]^{\beta}\right). \tag{7}$$

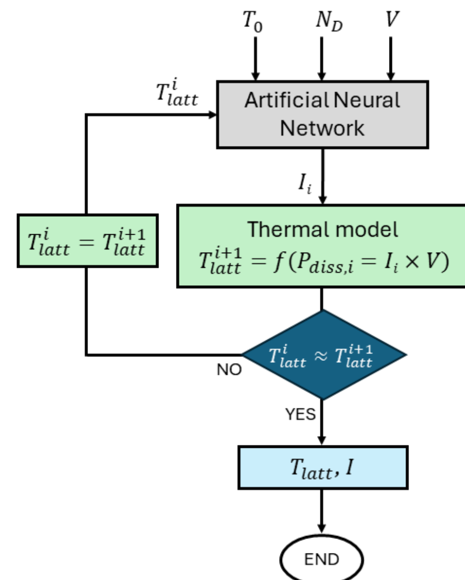

Fig. 5. Flux diagram of the combined ANN and thermal resistance models.

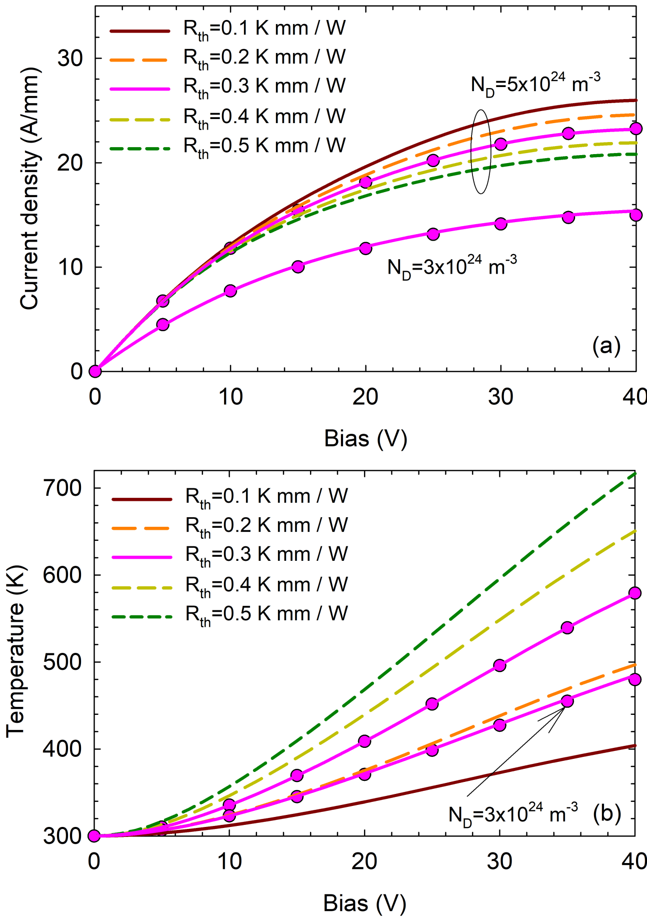

Fig. 6. (a) Current density and (b) lattice temperature vs. bias obtained with the combined ANN and the $TRM1$ for the values of R_{th}=0.1, 0.2, 0.3, 0.4 and 0.5 K· mm/W. T_{amb} = 300 K. Symbols represent results from MC electrothermal simulations using $TRM1$. Results are presented for N_D=5×10^{24} m^{-3} and N_D=3×10^{24} m^{-3}.

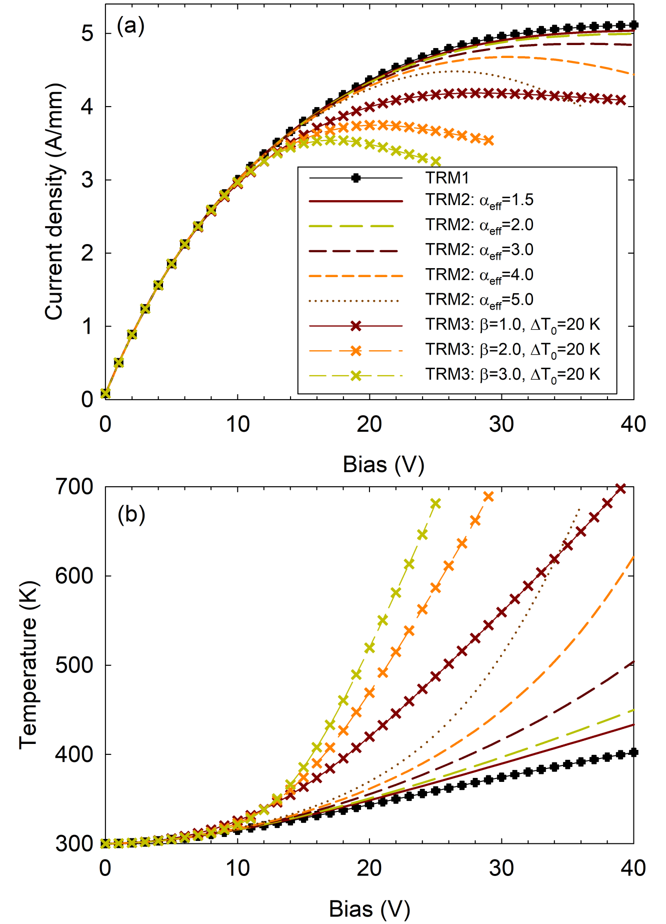

Fig. 7. (a) Current density and (b) lattice temperature vs. bias obtained with the combined ANN and the $TRM1$, $TRM2$ and $TRM3$ models for a value of R_{th}=0.5 K·mm/W. T_{amb} = 300 K. For the TRM2 α_{eff} is in the 1.5-5 range and for the TRM3 β is in the 1.0 - 3.0 range. N_D=5×10^{24} m^{-3}

The model considers the parameters β (which must be greater than or equal to 1), ΔT_0 and R_{th}, which depend on the geometry of the devices and surrounding areas, just as the thermal resistance does.

B. RESULTS AND DISCUSSION

Fig. 6(a) shows the current density obtained with $TRM1$ for five values of the thermal resistance in the 0.1 - 0.5 K·mm/W range (well within the range of values considered in our previous work [12]) to analyse the effect of self-heating. The predicted current density does not change significantly with R_{th} for low bias because P_{diss} is small, as well as the increase of T_{latt}, as can be observed in Fig. 6(b). For biases higher than 10 V the increase in temperature begins to be significant, having a notable effect on the current level, which takes decreasing values for larger R_{th}. We also have validated our combined ANN and thermal model by comparing its predictions for the cases of doping levels of N_D=3×10^{24} m^{-3} and N_D=5×10^{24} m^{-3} with the results directly obtained with an electrothermal MC simulator (symbols) incorporating $TRM1$ with a value of the thermal resistance R_{th}=0.3 K·mm/W. As can be observed, a very good agreement is found, for both the current density and T_{latt}.

The predicted current densities and lattice temperatures obtained with the combined ANN and the $TRM1$, $TRM2$ and $TRM3$ models are plotted in Figs. 7(a) and (b), respectively. In all cases a thermal resistance R_{th}=0.5 K·mm/W has been considered. For the $TRM2$ the value of α_{eff} has been varied in the 1.5-5 range according to those used in literature [12], [50], [51], [52], [53], [54]. The $TRM2$ introduces a non-linear response in the calculated T_{latt} respect to the applied bias, V. Finally, the $TRM3$ is employed taking into account ΔT_0=20 K and β in the 1.0 - 3.0 range [12]. As can be seen in Fig. 7, the $TRM3$ introduces a stronger self-heating effect, approximately from 12 V onwards. Moreover, applying this model the network temperature would be above 700 K for applied voltages starting from 39 V, 29 V and 25 V, for β=1 , 2 and 3, respectively, being, therefore, the limiting cases of validity of the model since the ANN has been trained up to 700 K and it is not valid to make predictions above this temperature.

V. CONCLUSIONS

A method based on an ANN trained with isothermal MC simulations and different power dissipation-dependent thermal models has been developed to predict T_{latt} and the current density in electronic devices. This model has been validated with electrothermal MC simulations, with good agreement in the results. The model is versatile as the ANN could be trained by considering more parameters as inputs, such as device geometry or material properties. The procedure could be applied to any thermal model where the temperature of the network depends on the dissipated power. Considering the proposed model, the computational cost will be considerably reduced compared to electrothermal MC simulations.

REFERENCES

[1] F. Roccaforte and M. Leszczynski, *Nitride Semiconductor Technology: Power Electronics and Optoelectronic Devices*. John Wiley & Sons, 2020.

[2] A. Hassan, Y. Savaria, and M. Sawan, "GaN integration technology, an ideal candidate for high-temperature applications: A review," *IEEE Access*, vol. 6, pp. 78 790–78 802, 2018.

[3] H. Klemm, "Silicon nitride for high-temperature applications," *Journal of the American Ceramic Society*, vol. 93, no. 6, pp. 1501–1522, 2010.

[4] J. Kuzmik, M. Ťapajna, L. Valik, M. Molnar, D. Donoval, C. Fleury, D. Pogany, G. Strasser, O. Hilt, F. Brunner *et al.*, "Self-heating in GaN transistors designed for high-power operation," *IEEE Transactions on Electron Devices*, vol. 61, no. 10, pp. 3429–3434, 2014.

[5] W. Tan, M. Uren, P. Fry, P. Houston, R. Balmer, and T. Martin, "High temperature performance of AlGaN/GaN HEMTs on Si substrates," *Solid-State Electronics*, vol. 50, no. 3, pp. 511–513, 2006.

[6] S. Singhal, T. Li, A. Chaudhari, A. W. Hanson, R. Therrien, J. Johnson, W. Nagy, J. Marquart, P. Rajagopal, J. C. Roberts *et al.*, "Reliability of large periphery GaN-on-Si HFETs," *Microelectronics Reliability*, vol. 46, no. 8, pp. 1247–1253, 2006.

[7] J. Würfl, V. Abrosimova, J. Hilsenbeck, E. Nebauer, W. Rieger, and G. Tränkle, "Reliability considerations of III-nitride microelectronic devices," *Microelectronics Reliability*, vol. 39, no. 12, pp. 1737–1757, 1999.

[8] A. Letellier, M. R. Dubois, J. P. Trovao, and H. Maher, "Gallium nitride semiconductors in power electronics for electric vehicles: Advantages and challenges," in *2015 IEEE vehicle power and propulsion conference (VPPC)*. IEEE, 2015, pp. 1–6.

[9] M. Rosker, C. Bozada, H. Dietrich, A. Hung, D. Via, S. Binari, E. Vivierios, E. Cohen, and J. Hodiak, "The DARPA wide band gap semiconductors for RF applications (WBGS-RF) program: Phase II results," *CS ManTech*, vol. 1, pp. 1–4, 2009.

[10] J. Mateos, S. Pérez, D. Pardo, and T. González, "Monte Carlo analysis of thermal effects in GaN HEMTs," in *2009 Spanish Conference on Electron Devices*. IEEE, 2009, pp. 459–462.

[11] S. García, I. Íñiguez-de-la Torre, O. García-Pérez, J. Mateos, T. González, P. Sangaré, C. Gaquière, and S. Pérez, "Self-consistent electro-thermal simulations of AlGaN/GaN diodes by means of Monte Carlo method," *Semiconductor Science and Technology*, vol. 30, no. 3, p. 035001, 2015.

[12] S. García-Sánchez, I. Íñiguez-de-la Torre, S. Pérez, K. Ranjan, M. Agrawal, R. Lingaparthi, D. Nethaji, K. Radhakrishnan, S. Arulkumaran, G. I. Ng *et al.*, "Non-linear thermal resistance model for the simulation of high power GaN-based devices," *Semiconductor Science and Technology*, vol. 36, no. 5, p. 055002, 2021.

[13] T. Sadi, R. W. Kelsall, and N. J. Pilgrim, "Investigation of self-heating effects in submicrometer GaN/AlGaN HEMTs using an electrothermal Monte Carlo method," *IEEE Transactions on Electron Devices*, vol. 53, no. 12, pp. 2892–2900, 2006.

[14] F. Bonani and G. Ghione, "On the application of the Kirchhoff transformation to the steady-state thermal analysis of semiconductor devices with temperature-dependent and piecewise inhomogeneous thermal conductivity," *Solid-State Electronics*, vol. 38, no. 7, pp. 1409–1412, 1995.

[15] W. Batty, C. E. Christoffersen, A. J. Panks, S. David, C. M. Snowden, and M. B. Steer, "Electrothermal CAD of power devices and circuits with fully physical time-dependent compact thermal modeling of complex nonlinear 3-D systems," *IEEE Transactions on Components and Packaging Technologies*, vol. 24, no. 4, pp. 566–590, 2001.

[16] A. J. McGaughey and M. Kaviany, "Quantitative validation of the Boltzmann transport equation phonon thermal conductivity model under the single-mode relaxation time approximation," *Physical Review B*, vol. 69, no. 9, p. 094303, 2004.

[17] H. Zhang, Y. Jing, and P. Zhou, "Machine learning-based device modeling and performance optimization for FinFETs," *IEEE Transactions on Circuits and Systems II: Express Briefs*, vol. 70, no. 4, pp. 1585–1589, 2022.

[18] S. García-Sánchez, R. Rengel, S. Pérez, T. González, and J. Mateos, "A Deep Learning-Monte Carlo combined prediction of side-effect impact ionization in highly doped GaN diodes," *IEEE Transactions on Electron Devices*, 2023.

[19] N. Hari, M. Ahsan, S. Ramasamy, P. Sanjeevikumar, A. Albarbar, and F. Blaabjerg, "Gallium nitride power electronic devices modeling using machine learning," *IEEE Access*, vol. 8, pp. 119 654–119 667, 2020.

[20] S. Zhao, F. Blaabjerg, and H. Wang, "An overview of artificial intelligence applications for power electronics," *IEEE Transactions on Power Electronics*, vol. 36, no. 4, pp. 4633–4658, 2020.

[21] L. Marquez, T. Hill, R. Worthley, and W. Remus, "Neural network models as an alternative to regression," in *Proceedings of the Twenty-Fourth Annual Hawaii International Conference on System Sciences*, vol. 4. IEEE, 1991, pp. 129–135.

[22] J. Bourquin, H. Schmidli, P. van Hoogevest, and H. Leuenberger, "Advantages of Artificial Neural Networks (ANNs) as alternative modelling technique for data sets showing non-linear relationships using data from a galenical study on a solid dosage form," *European Journal of Pharmaceutical Sciences*, vol. 7, no. 1, pp. 5–16, 1998.

[23] M. M. Mijwel, "Artificial neural networks advantages and disadvantages," *Mesopotamian Journal of Big Data*, vol. 2021, pp. 29–31, 2021.

[24] S. García, I. Íñiguez-de-la Torre, J. Mateos, T. González, and S. Pérez, "Impact of substrate and thermal boundary resistance on the performance of AlGaN/GaN HEMTs analyzed by means of electro-thermal Monte Carlo simulations," *Semiconductor Science and Technology*, vol. 31, no. 6, p. 065005, 2016.

[25] S. García-Sánchez, M. Abou Daher, M. Lesecq, L. Huo, R. Lingaparthi, D. Nethaji, K. Radhakrishnan, I. Íñiguez-De-La-Torre, B. Vasallo, S. Pérez *et al.*, "On the practical limitations for the generation of Gunn oscillations in highly doped GaN diodes," *IEEE Transactions on Electron Devices*, 2023.

[26] S. García, S. Pérez, I. Íñiguez-De-La-Torre, J. Mateos, and T. González, "Comparative Monte Carlo analysis of InP-and GaN-based Gunn diodes," *Journal of Applied Physics*, vol. 115, no. 4, 2014.

[27] S. Garcia-Sanchez, I. Íñiguez-de-la Torre, S. Perez, T. Gonzalez, and J. Mateos, "Optimization of the epilayer design for the fabrication of doped GaN planar Gunn diodes," *IEEE Transactions on Electron Devices*, vol. 69, no. 2, pp. 514–520, 2021.

[28] J. Mateos, T. González, D. Pardo, V. Hoël, and A. Cappy, "Monte Carlo simulator for the design optimization of low-noise HEMTs," *IEEE Transactions on Electron Devices*, vol. 47, no. 10, pp. 1950–1956, 2000.

[29] J. Mateos, T. González, I. Iniguez-De-La-Torre, S. García, S. Pérez, C. Gaquiere, G. Ducournau, M. Lesecq, M. Agrawal, and D. Nethaji, "Design and fabrication of planar Gunn nanodiodes based on doped GaN," *2019 IEEE Asia-Pacific Microwave Conference (APMC)*, pp. 971–973, 2019.

[30] C. Jacoboni and P. Lugli, *The Monte Carlo method for semiconductor device simulation*. Springer Science & Business Media, 2012.

[31] O. Madelung, *Semiconductors: data handbook*. Springer Science & Business Media, Berlin, 2004.

[32] M. Piccardo, L. Martinelli, J. Iveland, N. Young, S. P. DenBaars, S. Nakamura, J. S. Speck, C. Weisbuch, and J. Peretti, "Determination of the first satellite valley energy in the conduction band of wurtzite GaN by near-band-gap photoemission spectroscopy," *Physical Review B*, vol. 89, no. 23, p. 235124, 2014.

[33] S. Wu, P. Geiser, J. Jun, J. Karpinski, D. Wang, and R. Sobolewski, "Time-resolved intervalley transitions in GaN single crystals," *Journal of applied physics*, vol. 101, no. 4, 2007.

[34] J. Iveland, M. Piccardo, L. Martinelli, J. Peretti, J. W. Choi, N. Young, S. Nakamura, J. S. Speck, and C. Weisbuch, "Origin of electrons emitted into vacuum from ingan light emitting diodes," *Applied Physics Letters*, vol. 105, no. 5, 2014.

[35] T. Sadi, P. Kivisaari, J. Oksanen, and J. Tulkki, "On the correlation of the Auger generated hot electron emission and efficiency droop in III-N light-emitting diodes," *Applied Physics Letters*, vol. 105, no. 9, p. 091106, 09 2014.

[36] F. Bertazzi, M. Goano, X. Zhou, M. Calciati, G. Ghione, M. Matsubara, and E. Bellotti, "Looking for Auger signatures in III-nitride light

emitters: A full-band Monte Carlo perspective," *Applied Physics Letters*, vol. 106, no. 6, p. 061112, 02 2015.

[37] M. Goano, E. Bellotti, E. Ghillino, G. Ghione, and K. F. Brennan, "Band structure nonlocal pseudopotential calculation of the III-nitride wurtzite phase materials system. Part I. Binary compounds GaN, AlN, and InN," *Journal of Applied Physics*, vol. 88, no. 11, pp. 6467–6475, 12 2000.

[38] W. R. L. Lambrecht and B. Segall in, *Properties of group III nitrides / edited by James H. Edgar.*, ser. EMIS datareviews series ; no. 11. London: INSPEC, Institution of Electrical Engineers, 1994.

[39] J. Fang, M. V. Fischetti, R. D. Schrimpf, R. A. Reed, E. Bellotti, and S. T. Pantelides, "Electron transport properties of $\mathrm{Al}_x\mathrm{Ga}_{1-x}\mathrm{N}/\mathrm{GaN}$ transistors based on first-principles calculations and Boltzmann-Equation Monte Carlo simulations," *Phys. Rev. Appl.*, vol. 11, p. 044045, Apr 2019.

[40] I. Iñiguez-De-La-Torre, J. Mateos, T. González, D. Pardo, J. Galloo, S. Bollaert, Y. Roelens, and A. Cappy, "Influence of the surface charge on the operation of ballistic T-branch junctions: a self-consistent model for Monte Carlo simulations," *Semiconductor science and technology*, vol. 22, no. 6, p. 663, 2007.

[41] M.-C. Popescu, V. E. Balas, L. Perescu-Popescu, and N. Mastorakis, "Multilayer perceptron and neural networks," *WSEAS Transactions on Circuits and Systems*, vol. 8, no. 7, pp. 579–588, 2009.

[42] F. Murtagh, "Multilayer perceptrons for classification and regression," *Neurocomputing*, vol. 2, no. 5, pp. 183–197, 1991. [Online]. Available: https://www.sciencedirect.com/science/article/pii/0925231291900235

[43] A. B. Nassif, D. Ho, and L. F. Capretz, "Towards an early software estimation using log-linear regression and a multilayer perceptron model," *Journal of Systems and Software*, vol. 86, no. 1, pp. 144–160, 2013. [Online]. Available: https://www.sciencedirect.com/science/article/pii/S0164121212002221

[44] J. Heaton, *Introduction to neural networks with Java*. Heaton Research, Inc., 2008.

[45] "The Comprehensive R Archive Network," neuralnet: R package version 1.44.2. [Online]. Available: ttp://cran.r-project.org

[46] S. Patro and K. K. Sahu, "Normalization: A preprocessing stage," *arXiv preprint arXiv:1503.06462*, 2015.

[47] C. J. Willmott and K. Matsuura, "Advantages of the mean absolute error (MAE) over the root mean square error (RMSE) in assessing average model performance," *Climate research*, vol. 30, no. 1, pp. 79–82, 2005.

[48] J. Qi, J. Du, S. M. Siniscalchi, X. Ma, and C.-H. Lee, "On mean absolute error for deep neural network based vector-to-vector regression," *IEEE Signal Processing Letters*, vol. 27, pp. 1485–1489, 2020.

[49] J. Paasschens, S. Harmsma, and R. Van der Toorn, "Dependence of thermal resistance on ambient and actual temperature," in *Bipolar/BiCMOS Circuits and Technology, 2004. Proceedings of the 2004 Meeting*. IEEE, 2004, pp. 96–99.

[50] A. Sarua, H. Ji, K. Hilton, D. Wallis, M. J. Uren, T. Martin, and M. Kuball, "Thermal boundary resistance between GaN and substrate in AlGaN/GaN electronic devices," *IEEE Transactions on electron devices*, vol. 54, no. 12, pp. 3152–3158, 2007.

[51] S. Vitanov, V. Palankovski, S. Maroldt, and R. Quay, "High-temperature modeling of algan/gan hemts," *Solid-State Electronics*, vol. 54, no. 10, pp. 1105–1112, 2010.

[52] V. Sodan, S. Stoffels, H. Oprins, S. Decoutere, F. Altmann, M. Baelmans, and I. De Wolf, "Fast and distributed thermal model for thermal modeling of GaN power devices," *IEEE Transactions on Components, Packaging and Manufacturing Technology*, vol. 8, no. 10, pp. 1747–1755, 2018.

[53] C. Mion, J. Muth, E. Preble, and D. Hanser, "Accurate dependence of gallium nitride thermal conductivity on dislocation density," *Applied Physics Letters*, vol. 89, no. 9, 2006.

[54] D. Morelli, J. Heremans, and G. Slack, "Estimation of the isotope effect on the lattice thermal conductivity of group IV and group III-V semiconductors," *Physical Review B*, vol. 66, no. 19, p. 195304, 2002.